Journal of the Korean Nuclear Society
Volume 34, Number 3, pp.211~217, June, 2002

Development and High Power RF Test of the Vacuum Feedthrough for KSTAR ICRF Antenna

Young-Dug BAE, Churl Kew HWANG, and Jong-Gu KWAK
Korea Atomic Energy Research Institute
150 Dukjin-dong, Yuseung-gu, Daejon 305-353, Korea
ydbae@kaeri.re.kr

(Received October 15, 2001)

Abstract

A 1-MW vacuum feedthrough for the KSTAR ICRF antenna is fabricated and high power RF test is performed. It is designed to have two alumina(Al_2O_3) ceramic cylinders and O-ring seal instead of a brazed seal for good mechanical and thermal strength, which is important in long pulse or steady state operation. For cooling of the ceramics, dry air is circulated in a space between the two cylinders and the outer conductor. Independent cooling water channels are installed to cool the inner conductor of the feedthrough. RF high voltage test is performed using two kinds of ceramics with the purities of 99.7% and 97%. Stable operation is possible with the RF voltage of 30 kVp at long pulse of 300 sec without any severe damage.

Key Words : vacuum feedthrough, ICRF antenna, RF test, alumina ceramic

1. Introduction

Ion cyclotron range of frequency(ICRF) heating of fusion plasma is now being widely applied to fusion devices around the world.[1-3] Heating and current drive using fast wave in the ICRF range have been proposed as one of the main features for the advanced tokamak operation of the KSTAR(Korea Superconducting Tokamak Advanced Research) tokamak which has been constructed since 1995 as the major national fusion program.[4-5] The KSTAR ICRF system[6-7] has been designed to operate at any frequency in the range of 25~60 MHz and operate for a long pulse length up to 300 seconds. The ICRF system will deliver 6 MW of RF power to the plasma using a single four-strap antenna mounted in a mid-plane port, and it will be upgraded to 12 MW with the addition of a second system that is a duplicate of the first.

In the ICRF system, vacuum feedthrough is used for vacuum sealing between the pressurized transmission line and the evacuated transmission line. As the transmission power to the antenna through the vacuum feedthrough is MW level, it has to withstand the high RF voltage or the large RF current. It is a crucial component because its failure affects not only the RF system but also the entire machine vacuum integrity. For this purpose, several types of the vacuum feedthroughs have

been developed in the major laboratories.[8-12]

A 1-MW vacuum feedthrough has been developed in KAERI for several years to be used on the KSTAR ICRF system. It is designed to have two alumina(Al_2O_3) ceramic cylinders and O-ring seal instead of a brazed seal for good mechanical and thermal strength, which is important in long pulse or steady state operation. The electric field and resulting RF dissipation power are calculated to estimate long pulse capability. A prototype vacuum feedthrough was fabricated, and RF power test was performed at f=30 MHz.

2. Design and Fabrication of the Vacuum Feedthrough

The KSTAR ICRF antenna involving the vacuum feedthrough is shown in Fig.1. Eight vacuum feedthroughs are required per antenna. The vacuum feedthrough is located at the outside of the vacuum vessel for easy maintenance. Design requirement of the vacuum feedthrough for the KSTAR ICRF antenna is as follows.

1) A standoff voltage of 30 kV(rms) is required to transmit the RF power of 1 MW, and its current capability of 600 A(rms) is required.
2) It is designed to operate for a long pulse length up to 300 sec, and operate in the frequency range of 25 ~60 MHz.
3) The characteristic impedance of the vacuum side to be connected with 6" vacuum coax is 40 Ω and that of the pressurized side is 50 Ω.
4) The leak rate of the vacuum side should be lower than 9×10^{-7} Torr l /sec.

The vacuum feedthrough for the KSTAR ICRF antenna is designed as shown in Fig. 2. The feedthrough is made of two ceramic cylinders and has O-ring type vacuum seal instead of brazed seal, which is a unique design. The ceramic of the feedthrough is made with alumina(Al_2O_3). The

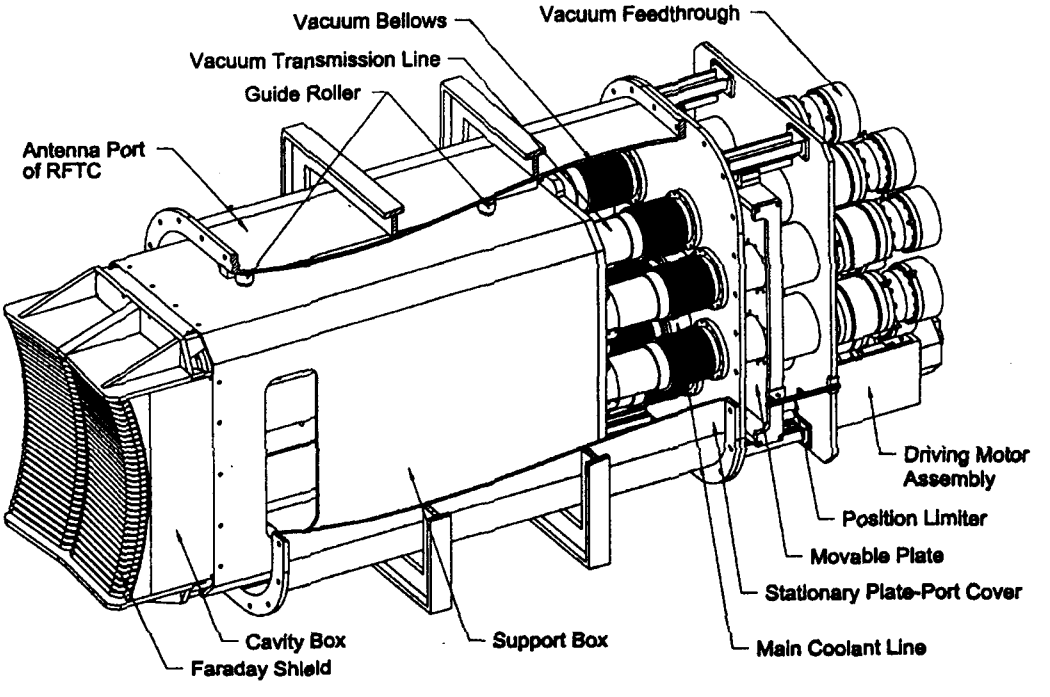

Fig. 1. 3-D Drawing of KSTAR ICRF Antenna

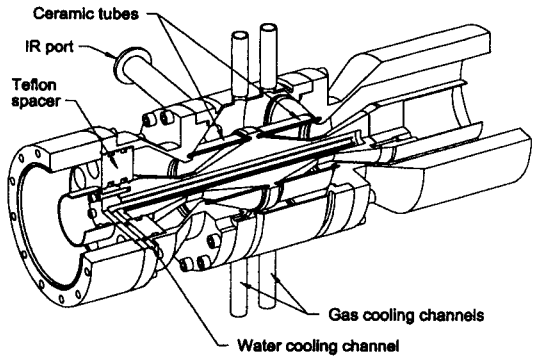

Fig. 2. Cut View of the Vacuum Feedthrough

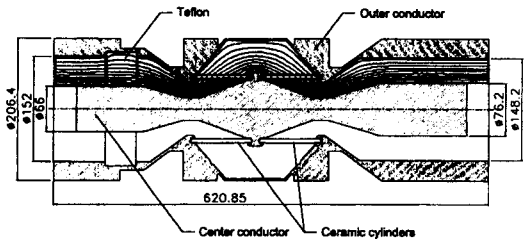

Fig. 3. Contours of Constant Potential

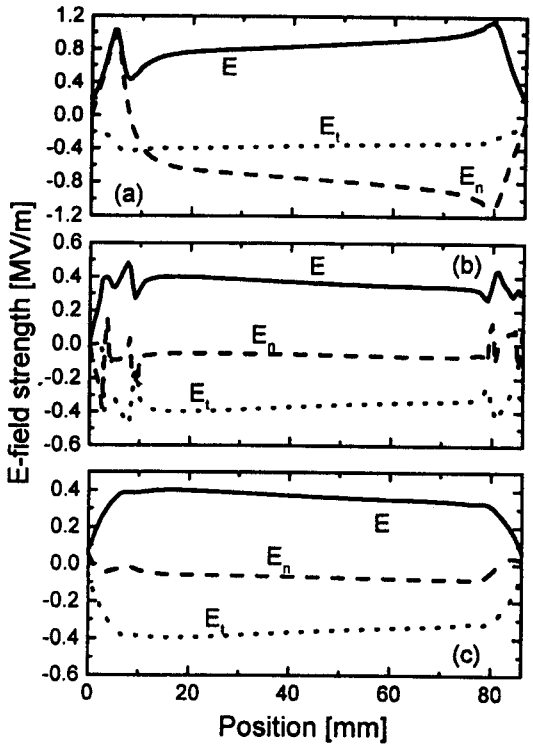

Fig. 4. Electric Field Strength on the Inner(a) /outer(b) Surfaces, and the Inside(c) of the Ceramics at V=30 kV of the Voltage Difference

ceramic cylinder has two narrow groves on the outer surface at both ends to enhance the breakdown strength. The center and outer conductors are shaped to reduce the component of the electric field along the surface of the ceramic. The possibility of surface breakdown can thereby be substantially reduced. Also, the shape of the conductors is optimized to minimize the electric field strength. The electric field strength is calculated in the space between the center and outer conductors using the commercial FEM code(Quick Field). In the case of a voltage difference of 30 kV, its result is shown in Figs. 3 and 4. The tangential component of the electric field, which is taken to be the limiting factor on the surface breakdown, is lower than 0.5 MV/m on both surfaces. The RF power dissipation due to the dielectric loss in the ceramic is given by

$$P_{RF} = \frac{1}{2}\,\varepsilon_0\varepsilon_r \tan\delta\,\omega \int\int 2\pi r E^2(r,z)\,dr\,dz, \quad (1)$$

where ε_r is the relative dielectric constant, $\tan\delta$ is the loss tangent of the ceramic, and E(r,z) is the rms value of the electric field strength at position (r,z). In this case, the power dissipation is obtained using the electric field strength inside the ceramic, shown in Fig. 4(c). For the alumina ceramic 86.5 mm long and 6 mm thick, when $\tan\delta = 5\times10^{-4}$, $\varepsilon_r = 10$, V=30 kV(rms), and $f=\omega/2\pi=50$ MHz, P_{RF} is calculated to be 260 W.

If no active cooling is provided for the ceramic, its temperature can be estimated by assuming the power absorbed in the ceramic is translated to the heating power for increasing internal energy and the radiation loss power. In this case, the power absorbed in the ceramic can be written

$$P_{RF} = \frac{MC_p(T-T_0)}{\Delta t} + \frac{\sigma A_1(T^4-T_2^4)}{1/e_1+\frac{A_1}{A_2}(1/e_2-1)}, \quad (2)$$

where M and C_p are the mass and specific heat of the ceramic, respectively; T_0 is the initial temperature of the ceramic; Δt is the pulse length; σ is Stefan-Boltzman constant; A_1 and A_2 are the surface areas of the ceramic and the outer conductor, respectively; T_2 is the temperature of the outer conductor; and e_1 and e_2 are the emmittances of the ceramic and the outer conductor, respectively. At a low temperature, the first term of Eq.(2) is higher than the second term. On the contrary, in the case of a steady state operation, the second term is higher than the first. If the temperature of the outer conductor can be maintained near room temperature, i.e. T_2=20℃, and initial temperature of the ceramic is T_0=20℃, T is calculated as shown in Fig. 5. In this calculation, we used nominal value of the emittances; e_1=0.5 and e_2=0.3. For the pulse length of 300 sec, the maximum temperature is 165℃ at f=50 MHz, which means that the active cooling is required to bring the temperature of the ceramic below the temperature limit of the Viton O-ring. At the maximum temperature of 165℃, the radiation loss term of Eq.(2) is lower than 6% of the internal energy term.

In the center conductor, RF power is dissipated by the Ohmic loss of RF current and the heat per unit surface area is given by

$$P_{loss} = R_s I^2 / (\pi d)^2 \quad (3)$$

where R_s is the surface resistance, and d is a diameter of the center conductor at the concerned position. The surface resistance is given by

$$Rs = \rho / \delta_s, \quad (4)$$

where ρ is the resistivity, and δ_s is the skin depth. In the case of Al6061, which is the material of the center conductor, the resistivity is 2.65×10^{-8} Ω m, and the skin depth is 11.6 μm at the frequency of 50 MHz. For the center conductor surfaces, the design requirement of the current, I=600 A is translated into

$$P_{loss} = 83.5/d^2. \quad (5)$$

Total power dissipated in the center conductor can be obtained by the integration of Eq.(5) along the surface of the center conductor. In this case, total power is 1kW, and the power dissipated on the surface of the minimum radius reaches up to 140W. In the same way, total power dissipated on the outer conductor is calculated to be 177W.

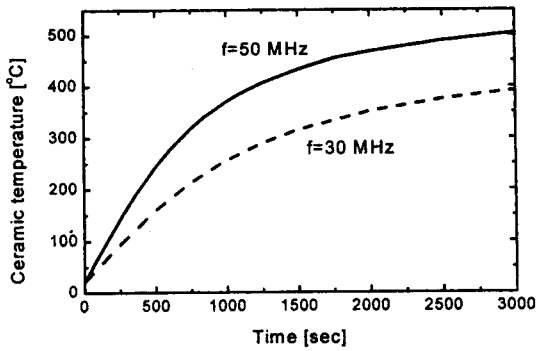

Fig. 5. Temperature Increase of the Ceramic Due to the Dielectric Loss

For the long pulse operation, the feedthrough has a water-cooling channel inside the center conductor. Also, it has forced gas-cooling channels in order to remove the dielectric heat loss in the ceramic material. The cooling gas is injected into the ceramic surface through two outer nozzles.

On the basis of the above design, the vacuum feedthrough was fabricated and its photograph is shown in Fig. 6. In this study, two kinds of ceramic cylinders with identical dimensions were used. They were fabricated by two independent companies; the first has high purity of 99.7%(named 'ceramic-A' in this study), and the second has a relatively

Fig. 6. Vacuum Feedthrough Installed on the Test Stand

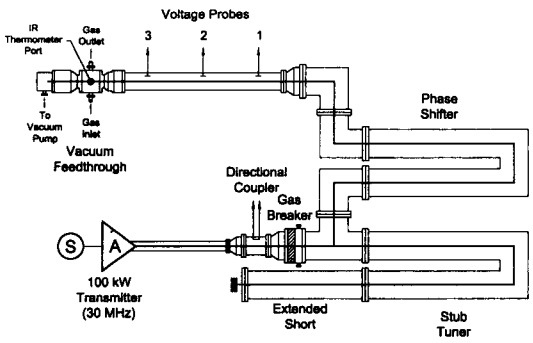

Fig. 7. High Power RF Test Stand Schematic

low purity of 97% (ceramic-B). The helium leak rate in the vacuum side of the feedthrough was measured to be 5.2×10^{-9} Torr · l /sec which satisfies the design requirement. The water-cooling channel was tested using pressurized water at 10 kgf/cm^2.

3. High Power RF Test

The RF power test of the vacuum feedthrough was accomplished at f=30 MHz using the experimental apparatus shown schematically in Fig. 7. The feedthrough is placed at the end of the test section, and its end is electrically opened, which means that the voltage at the feedthrough position becomes maximum. It is connected to the matching circuit through the pressurized transmission line in which three voltage probes are installed. The matching circuit consists of a phase shifter and a stub tuner, which are both trombone type. The matched line section from stub tuner to vacuum feedthrough is pressurized with N_2 gas at 2kgf/cm^2 to increase stand-off voltage. The matching circuit is connected to the RF transmitter through the dual directional coupler. The transmitter has the power capability of 100kW CW, and its operation range of frequency is 30± 0.5MHz. In this test, dry air was injected into the ceramic surface through two outer nozzles with the flow rate of 200 LPM, but the cooling water was not led to the center conductor. The temperature of the ceramic cylinder was measured by IR thermometer. During the RF pulse, the line voltage, the forward/reflected powers, the temperature of the ceramic, and the gas pressure in the vacuum chamber were measured. The temperature of the transmission line was monitored at several points.

The RF power test for the vacuum feedthrough with the ceramic-A was performed up to 30.2 kV(peak) at a pulse length of 60 sec. Time evolutions of RF pulse, the line voltage, the temperature, and the gas pressure are shown in Fig. 8. The maximum voltage of the standing wave was limited by the output power of the amplifier and the circuit loss. The pulse length was limited by the overheating of the ceramic which is named 'ceramic-A'. The temperature of the ceramic-A increased up to 112℃(T_0=30℃), which is much higher than the expected value of 39℃. It may be caused by the fact that the tanδ of the ceramic-A is abnormally high. From this experimental result, the tanδ of the ceramic-A is estimated to be 5×10^{-3}, one order higher than the nominal value of 5×10^{-4}. Multipactor discharge occurred at the beginning phase of the RF pulse and it was terminated as the

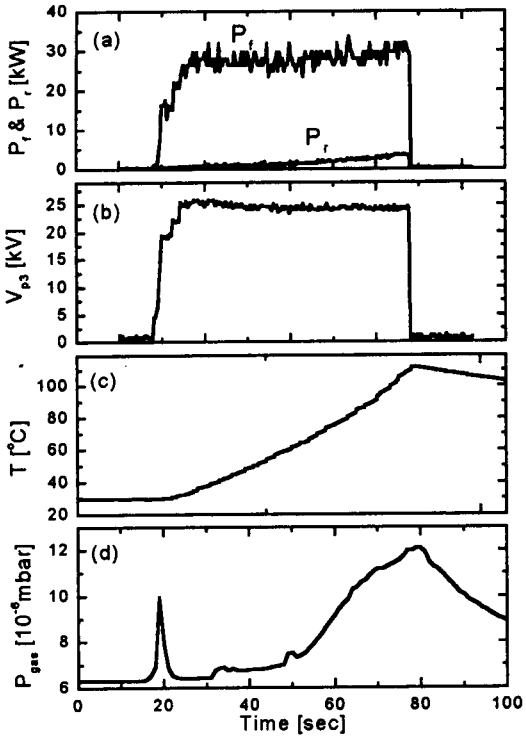

Fig. 8. Time Evolution of Forward and Reflected Powers(a), Line Voltage at V-probe #3(b), Temperature of the Ceramic-A(c), and Gas Pressure in the Vacuum Chamber(d)

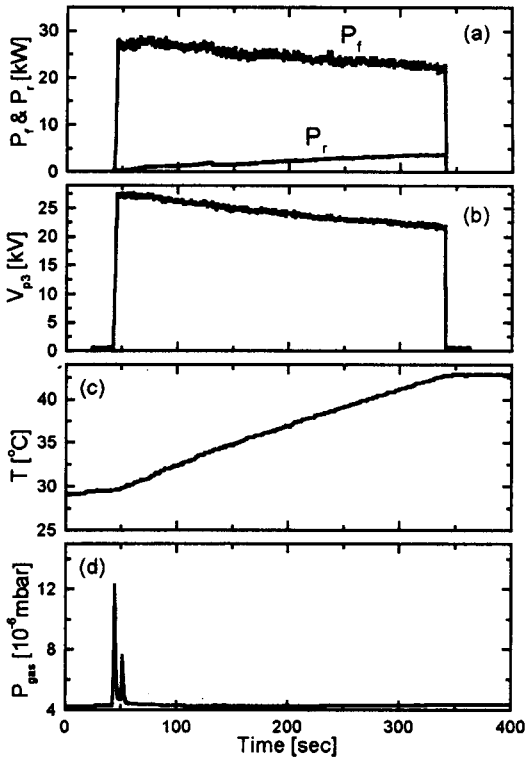

Fig. 9. Time Evolution of Forward and Reflected Powers(a), Line Voltage at V-probe #3(b), Temperature of the Ceramic-B(c), and Gas Pressure in the Vacuum Chamber(d)

forward power increased. Thereby there is a narrow peak of the gas pressure in the multipactor region, as shown in Fig. 8(d). After the multipactor discharge was terminated, the gas pressure increased by the surface conditioning. The reflected power increased gradually during the RF pulse, which is caused by the temperature effect. However the reflected power was maintained to be less than 17% of the forward power, and the VSWR was lower than 2.5.

For the vacuum feedthrough with the ceramic-B, a similar test was performed. Time evolutions of RF pulse, the line voltage, the temperature, and the gas pressure are shown in Fig. 9. The forward power decreased and the reflected power increased gradually during the RF pulse, because the matching condition of the test circuit was shifted from the optimum condition by the heating of the transmission line components. The maximum voltage of the standing wave was 32.2 kV(peak) and the pulse length was extended to 300 sec with the temperature increase of only up to 43℃ (T_0=30℃), which is much lower than that of the ceramic-A. It means that the tanδ of the ceramic-B is much lower than that of the ceramic-A. From the experimental result, the tanδ of the ceramic-B is estimated to be 2×10^{-4}, which is a satisfactorily low value. The maximum peak voltage of 30kV is equivalent to a 0.8MW transmission power to the antenna with 6 Ω/m of expected plasma loading. It

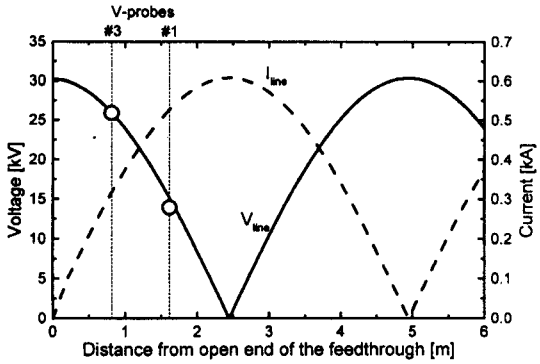

Fig. 10. Voltage and Current vs Distance from Open End of the Feedthrough. Two Open Circles Denote the Measured Voltage

means that total power of 6.1MW can be delivered to the plasma, which fulfills the design requirement. Standing wave voltage and current along the line are shown in Fig. 10 with the maximum peak voltage of 30 kV.

4. Conclusions

The vacuum feedthrough was designed and fabricated for the KSTAR ICRF antenna. The RF power test of the feedthrough was performed at f=30MHz. The feedthrough has a good performance up to a RF voltage of 30kVp at a long pulse of 300 sec without any severe damage. It is known that the key parameter of the ceramic insulator is low tanδ rather than high purity. In future works, a high current test will be performed with the electrical-short end of the vacuum feedthrough.

Acknowledgements

This work was supported by the Korea Ministry of Science and Technology under the KSTAR Project Contract.

References

1. G. Bosia, M. Makowski and G.Tonon, Plasma Phys. Control. Fusion, 40, A105 (1998).
2. M. Saigusa, T. Fujii, H. Kimura, S. Moriyama, K.Annoh, M. Terakado, and N. Kobayashi, Fusion Engineering and Design, 24, 47 (1994).
3. A. Kaye, J. Jacquinot, P. Lallia, and T. Wade, Fusion Technology, 11, 203 (1987).
4. G.S. Lee et. al., Nuclear Fusion, 40, 575 (2000).
5. B.G. Hong, J. Korean Phys. Soc., 36, 90 (2000).
6. B.G. Hong, Y.D. Bae, C.K. Hwang, J.G. Kwak, M.H. Ju, D.W. Swain, P.M. Ryan and B.W. Riemer, Proc. of the 20th SOFT, Vol.1, p. 303 (1988).
7. C.K. Hwang, B.G. Hong, and D. Swain, Fusion Engineering and Design, 45, 127 (1999).
8. H. Welder, F. Wesner, W. Becker, and R. Fritsch, Fusion Engineering and Design, 24, 75 (1994).
9. JAERI, JAERI Report No. JAERI-memo 63-039 (1988).
10. A. Kaye, T. Brown, V. Bhatnagar, P. Crawley, J. Jacquinot, R. Lobel, J. Plancoulaine, P.H. Rebut, T. Wade, and C. Walker, Fusion Engineering and Design, 24, 1 (1994).
11. T. Mutoh, R. Kumazawa, T. Seki. F. Simpo, G. Nomura, T. Ido, and T. Watari, NIFS Report No. NIFS-552 (1998).
12. T.L. Owens, F.W. Baity, D.J. Hoffman, and J.H. Whealton, Fusion Technology, 8, 381 (1985).